DOI:10.1021/jf903000c

JOURNAL OF AGRICULTURAL AND FOOD CHEMISTRY
ARTICLE

^{18}O Stable Isotope Labeling, Quantitative Model Experiments, and Molecular Dynamics Simulation Studies on the Trans-Specific Degradation of the Bitter Tasting Iso-α-acids of Beer

Daniel Intelmann,[†] Oliver Demmer,[‡] Nina Desmer,[§] and Thomas Hofmann*,[†]

[†]Chair of Food Chemistry and Molecular Sensory Science, Technische Universität München, Lise-Meitner Strasse 34, D-85354 Freising, Germany, [‡]Department of Chemistry, Organic Chemistry II, Technische Universität München, Lichtenbergstrasse 4, D-85747 Garching, Germany, and [§]Institute of Food Chemistry, Westfälische-Wilhelms Universität Münster, Corrensstrasse 45, D-48149 Münster, Germany

The typical bitterness of fresh beer is well-known to decrease in intensity and to change in quality with increasing age. This phenomenon was recently shown to be caused by the conversion of bitter tasting *trans*-iso-α-acids into lingering and harsh bitter tasting tri- and tetracyclic degradation products such as tricyclocohumol, tricyclocohumene, isotricyclocohumene, tetracyclocohumol, and epitetracyclocohumol. Interestingly, the formation of these compounds was shown to be trans-specific and the corresponding *cis*-iso-α-acids were found to be comparatively stable. Application of ^{18}O stable isotope labeling as well as quantitative model studies combined with LC−MS/MS experiments, followed by computer-based molecular dynamics simulations revealed for the first time a conclusive mechanism explaining the stereospecific transformation of *trans*-iso-α-acids into the tri- and tetracyclic degradation products. This transformation was proposed to be induced by a proton-catalyzed carbon/carbon bond formation between the carbonyl atom C(1′) of the isohexenoyl moiety and the alkene carbon C(2″) of the isoprenyl moiety of the *trans*-iso-α-acids.

KEYWORDS: Iso-α-acids; tricyclocohumol; tricyclocohumene; isotricyclocohumene; tetracyclocohumol; epitetracyclocohumol; stable isotope labeling

INTRODUCTION

Made from water, barley malt, yeast, and hops (*Humulus lupulus* L.), a freshly brewed beer has been attracting consumers for thousand of years due to its refreshing character, desirable aroma, and its typical bitter taste profile. Based on the outcome of about 100 years of research on the molecules contributing to the typical flavor signature of beer, it can be concluded that the bitter taste of the beverage develops upon isomerization of the α-acids cohumulone (**1a**), humulone (**1b**), and adhumulone (**1c**) after addition of cones, pellets, or extracts of hop during the wort boiling process (**Figure 1**). The α-acids (**1**) are transformed into epimeric pairs of intensely bitter tasting cis- (**2**) and trans-configured iso-α-acids (**3**) (*1*) which were found to be vital for the typical taste of beer and exist in freshly brewed beer in a trans/cis ratio of about 0.4 (*2*−*6*). As a consequence of the three different alkanoyl side chains of the precursor α-acids, these iso-α-acids occur as trans- and cis-configured isocohumulone (**2a**, **3a**), isohumulone (**2b**, **3b**), and isoadhumulone (**2c**, **3c**), respectively.

Unfortunately, the attractive flavor of beer changes rapidly upon storage and limits the shelf life of the beverage. During recent decades, multiple studies investigated photooxidation as well as radical-assisted oxidation reactions leading to storage-induced off-flavor formation in the fraction of volatile aroma compounds (*7*−*13*). Besides the aroma, also the typical bitterness of fresh beer is well-known to decrease in intensity and to change in quality with increasing age (*14*−*17*). Interestingly, aging of beer was found to go in hand with the degradation of *trans*-iso-α-acids (**3**), whereas the *cis*-iso-α-acids (**2**) seem to be rather stable (*6*, *14*, *16*−*21*).

Although the depletion of *trans*-iso-α-acids upon storage of beer takes place under quasi oxygen-free conditions and in the absence of light, the degradation of *trans*-iso-α-acids is widely considered to be an oxidative process (*6*, *14*). There are only a few proposals on the structures of iso-α-acid degradation products as well as their underlying formation mechanisms such as, e.g., photolytic cleavage of the isohexenoyl side chain (*9*) or the alkali-catalyzed formation of humulinic acids (*22*, *23*). Although numerous publications proposed chemical structures of putative iso-α-acid degradation products, most of these model experiments have been done using rather artificial model conditions (*24*−*27*). Most important, the compounds previously identified do not at all explain the different reactivity of *trans*-iso-α-acids (**3**) and *cis*-iso-α-acids (**2**) as well as the trans-specificity formation of iso-α-acid degradation products.

To close this gap and to investigate the degradation of *trans*-iso-α-acids (**3**) and *cis*-iso-α-acids (**2**) in authentic beer samples, both isomers were very recently incubated in model solutions under comparative conditions and a series of previously not reported degradation products formed from *trans*-iso-α-acids (**3**) were successfully isolated and identified for the first time (*28*).

*To whom correspondence should be addressed. Phone: +49-8161-71-2902. Fax: +49-8161-71-2949. E-mail: thomas.hofmann@wzw.tum.de.

 Published on Web 10/27/2009

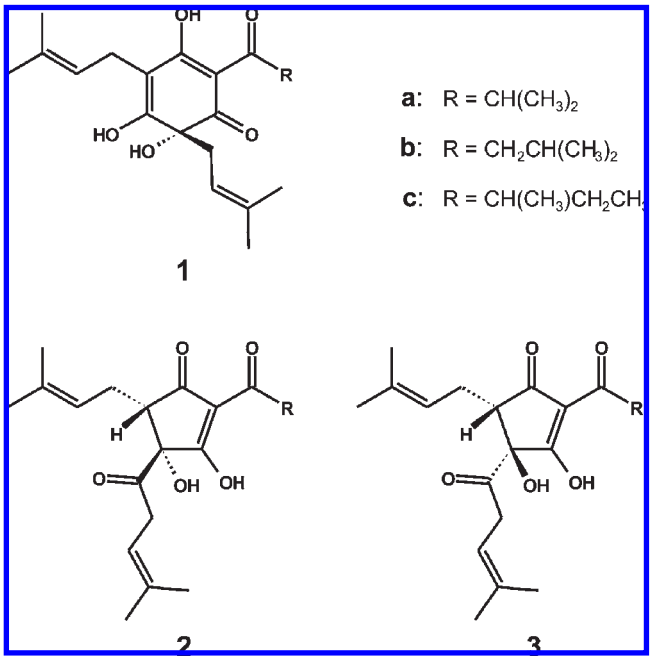

Figure 1. Structures of the α-acids cohumulone (**1a**), humulone (**1b**), and adhumulone (**1c**) and the isomerization products *cis*- (**2a**) and *trans*-isocohumulone (**3a**), *cis*- (**2b**) and *trans*-isohumulone (**3b**), and *cis*- (**2c**) and *trans*-isoadhumulone (**3c**) formed upon wort boiling.

As an example, *trans*-isocohumulone (**3a**), but not the corresponding cis isomer (**2a**), was found to produce the lingering and harsh bitter tasting transformation products tricyclocohumol (**4a**), tricyclocohumene (**5a**), isotricyclocohumene (**6a**), tetracyclocohumol (**7a**), and epitetracyclocohumol (**8a**) upon storage in hydroalcoholic solution (**Figure 2**). Most interestingly, the formation of such degradation products could not be observed when *cis*-iso-α-acids (**2**) were used in the model storage experiment (*28*), thus being well in line with the stability of *cis*-iso-α-acids (**2**) observed during storage of beer (*6*, *14*, *16*−*21*).

Although the structures of the compounds **4a**−**8a** have been verified in beer samples (*28*), the mechanism explaining their stereospecific formation from *trans*-iso-α-acids is yet not clear. The objective of the present study was, therefore, to elucidate the formation pathway of the compounds **4a**−**8a** from *trans*-iso-α-acids (**2**) by means of quantitative model studies, ^{18}O stable-isotope labeling experiments, and a molecular dynamics simulation, and to investigate their formation during storage of authentic beer samples.

MATERIALS AND METHODS

Chemicals and Materials. The following chemicals were obtained commercially: formic acid, hydrochloric acid, and sodium hydroxide (Grüssing, Filsum, Germany); acetonitrile, ethylacetate, ethanol (Merck, Darmstadt, Germany); dicyclohexylamine was of puriss. grade (Fluka, Neu-Ulm, Germany). ^{18}O-labeled water (isotopic abundance >98%) was from Euriso-top (Saarbrücken, Germany). Deionized water used for chromatography was purified by means of a Milli-Q Gradient A10 system (Millipore, Billerica, MA). Commercial Pilsner-type beer samples were obtained from the German brewing industry. In order to study the influence of forced aging, canned beer samples were maintained at 6, 27, and 37 °C for up to 18 weeks prior to opening and subsequent analysis.

Following a literature protocol (*21*), *cis*- and *trans*-iso-α-acids (**2a**−**3c**) were isolated from a commercially available iso-α-acid extract (Hallertauer Hopfenveredelungsgesellschaft mbH, Mainburg, Germany) in a purity of more than 98% (HPLC, ^1H NMR). Reference compounds of the *trans*-iso-α-acid degradation products tricyclocohumol (**4a**), tricyclocohumene (**5a**), isotricyclocohumene (**6a**), tetracyclocohumol (**7a**), epitetracyclocohumol (**8a**), tricyclohumol (**4b**), tricyclohumene (**5b**), isotricyclohumene (**6b**), and tetracyclohumol (**7b**) were prepared in a purity of more than 97% (HPLC, ^1H NMR) as reported recently (*28*).

Iso-α-acid Spiking and Forced Aging of Beer. Aliquots (20 mL each) of a fresh beer sample were placed into brown-glass vials (25 mL) under an atmosphere of nitrogen and, then, spiked with an ethanolic solution (250 μL) of *cis*-isohumulone (**2b**, 2.6 mmol/L), *trans*-isohumulone (**3b**, 3.0 mmol/L), or ethanol (250 μL, control sample). Thereafter, the vials were sealed, maintained for 14 days at 37 °C in the dark, and then analyzed by means of HPLC−MS/MS using the multiple reaction monitoring (MRM) mode.

^{18}O Stable Isotope Labeling Experiments. Two types of ^{18}O-labeling experiments were performed. First, an $^{16}O/^{18}O$ isotope exchange experiment (expt A) was performed in order to determine those oxygen atoms in the target molecule which do exchange with water. To achieve this, samples (300 μg) of *trans*-isohumulone (**3b**), tricyclohumol (**4b**), tricyclohumene (**5b**), isotricyclohumene (**6b**), or tetracyclohumol (**7b**), respectively, were dissolved in $H_2{}^{18}O$ (150 μL), the pH value was adjusted to pH 4.0 with trace amounts of concentrated hydrochloric acid, and then the samples were incubated at 37 °C in screwed glass vials. After 2 h, the solutions were cooled to room temperature and adjusted to a final concentration of 0.1 μmol/L by the addition of acetonitrile. Using a syringe pump (flow rate: 10 μL/min), the sample solutions were directly injected into the mass spectrometer operated in the negative electrospray ionization mode. The ratio of the isotopologues of the corresponding target compounds was determined using the $Q1^-$ scan mode and the fragmentation pattern was obtained by applying collision-activated dissociation (CAD) in the product ion mode (MS^2).

A second set of experiments (expt B) was performed in order to locate stably incorporated oxygen atoms in the transformation products **4b**−**8b** generated during storage of *trans*-iso-α-acids. To achieve this, a solution of *trans*-isohumulone **3b** (30 μmol/L) in $H_2{}^{18}O$ (250 μL) was adjusted to pH 2.0 by adding trace amounts of concentrated hydrochloric acid and, then, kept for 4 h at 60 °C in the dark. After cooling to room temperature, the solvent was removed in vacuum and the residue was taken up in H_2O (250 μL) to wash out exchangeable ^{18}O atoms. In order to study the presence of stable-bound ^{18}O atoms in the degradation products formed, these solutions were used for LC−MS/MS scan and fragmentation experiments.

Influence of the pH Value on *trans*-Iso-α-acid Degradation. Aqueous solutions (each 1.0 mL, 10 μmol/L) of *trans*-isocohumulone (**3a**) adjusted to pH 1.0, 3.0, 4.0, and 6.0, respectively, were maintained at 60 °C for up to 72 h in the dark. After regular time intervals, an aliquot (100 μL) of the solution was withdrawn with a syringe and analyzed for *trans*-isocohumulone (**3a**) as well as the degradation products tricyclocohumol (**4a**), tricyclocohumene (**5a**), isotricyclocohumene (**6a**), tetracyclocohumol (**7a**), and epitetracyclocohumol (**8a**) by means of HPLC−MS/MS analysis running in the MRM mode.

Mass Spectrometry (LC−MS/MS). An Agilent 1100 series HPLC−system consisting of a pump, a degasser, and an autosampler (Agilent, Waldbronn, Germany), or alternatively a PHD 4400 Hpsi-type syringe pump (Harvard Apparatus, Holliston, MA) was connected to an API 4000 Q-TRAP mass spectrometer (AB Sciex Instruments, Darmstadt, Germany) which was equipped with an electrospray ionization (ESI) source operating in the negative ion mode. For HPLC−MS/MS experiments, nitrogen was used as turbo gas at 400 °C. The compound-specific declustering potential (DP), cell exit potential (CXP), and collision energy (CE) were optimized for each substance prior to the analysis by infusion of pure reference solutions and are summarized in **Table 1**. The dwell time for each mass transition was 44 ms. For direct infusion experiments using the syringe pump, no additional turbo gas was used. The ion spray voltage was set to −4500 V. Data acquisition and processing was performed by using the Analyst software version 1.4.2 (AB Sciex Instruments, Darmstadt, Germany).

For quantitative analysis of iso-α-acids and their degradation products in beer samples as well as model experiments by means of HPLC−MS/MS, a 150 × 2 mm, 5 μm, Pursuit C18 column (Varian, Middelburg, The Netherlands) was used as the stationary phase and a gradient of acetonitrile containing 0.5% formic acid (solvent A) and aqueous formic acid (0.5% in water; solvent B) were used as the mobile phase. Using a flow rate of 250 μL/min, chromatography was performed by increasing solvent A from 5 to 10% within 15 min, then to 61% within 37 min, to 65% within 13 min, to 100% within 15 min, holding 100% for 5 min, and, finally,

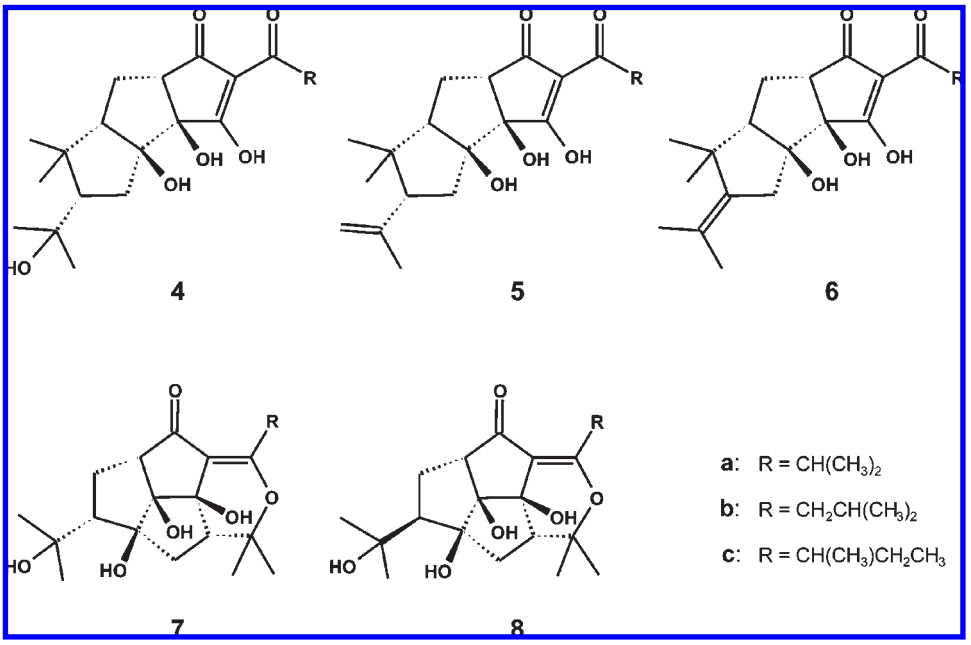

Figure 2. Chemical structures of the recently identified *trans*-iso-α-acid degradation products **4**−**8**. As an example, tricyclohumol (**4b**), tricyclohumene (**5b**), isotricyclohumene (**6b**), tetracyclohumol (**7b**), and epitetracyclohumol (**8b**) are generated from *trans*-isohumulone (**3b**).

Table 1. Optimized Mass Spectrometric Parameters for the Quantitative Analysis of Iso-α-acids (**2**, **3**) and Their Degradation Products **4**−**8**

compound no.[a]	mass transition[b]	DP[c] [V]	CE[d] [V]	CXP[e] [V]
2a, **3a**	*m*/*z* 347.0 → 251.0	−90	−22	−11
2b/**c**, **3b**/**c**	*m*/*z* 361.0 → 265.0	−90	−22	−11
4a	*m*/*z* 365.3 → 165.0	−105	−48	−9
4b/**c**	*m*/*z* 379.3 → 179.0	−105	−48	−9
5a, **6a**	*m*/*z* 347.2 → 165.0	−60	−52	−7
5b/**c**, **6b**/**c**	*m*/*z* 361.2 → 179.0	−60	−52	−7
7a, **8a**	*m*/*z* 365.3 → 193.1	−120	−46	−11
7b/**c**, **8b**/**c**	*m*/*z* 379.3 → 207.1	−120	−46	−11

[a] Structures and numbering of compounds refer to **Figures 1** and **2**. [b] Mass transition selected for quantitative analysis by means of LC−MS/MS. [c] Declustering potential. [d] Collision energy. [e] Cell exit potential.

decreasing within 5 min to 5%. Prior to the injection of the sample (5 μL), the system was equilibrated for 5 min.

Analysis of the ratio of individual isotopologues in the ^{18}O-labeling experiment was performed by MS scan experiments. Using a flow rate of 10 μL/min, the sample solution was introduced into the mass spectrometer and, after ionization in the ESI source applying a declustering potential (DP) of −60 V, a mass range from 300 to 500 amu was scanned in Q1. Each scan cycle was measured within 1 s. Isotopic ratios were determined as averages of at least 10 scans.

For the analysis of the MS/MS fragmentation of target compounds, the sample was infused into the mass spectrometer with a flow rate of 10 μL/min. After ionization in the ESI source (DP = −60 V), distinct masses were selected by Q1 and subsequently fragmented in Q2 by collision-induced fragmentation using nitrogen at 4×10^{-5} Torr and a collision energy of −35 V. In Q3, fragment ions were scanned in a range from 100 to 400 amu. Each scan cycle was measured within 1 s. Fragmentation patterns were determined as averages of at least 10 scans.

For the analysis of isotope ratios and the MS/MS fragmentation pattern of target compounds from complex model mixtures, scan/fragmentation experiments were performed by means of HPLC−MS/MS using the chromatographic conditions detailed above. During HPLC analysis, eight individual MS/MS experiments were performed simultaneously with the ions *m*/*z* 361, 363, 365, 367, 379, 381, 383, and 385, which were calculated from the molecular mass of the pseudomolecular ion of each target compound (361 amu for **3b**, 379 amu for **4b** and **7b**) plus the isotopic shift of 2, 4, 6, and 8 amu induced by the incorporation of one, two, three, or four ^{18}O atoms, respectively. For each of these calculated ions, their corresponding fragment ions were recorded.

Molecular Dynamics Simulation. The GROMACS 4.0.3 software package (www.gromacs.org) was used to perform the MD simulations (*29*, *30*). All scripts for subsequent analysis were packaged with GROMACS. The software packages VMD (*31*) and PyMOL (www.pymol.org) were used for visualization of the trajectories. The OPLS-AA force field was used for the molecular dynamics simulations. Rigid SPC water was the water model used. Remaining solute bonds were constrained by the SHAKE algorithm and temperature, and pressure control was executed by Berendsen coupling (*32*). A cubic simulation box with periodic boundary conditions was employed, along with PME (rcoulomb = 1.1 nm) for electrostatic and with a cutoff distance (rvdw = 1.1 nm) for Lennard-Jones nonbonding interactions.

The MD simulations were established and performed using the following procedure. The molecules were built with SYBYL 7.3 (Tripos International, St. Louis, MO), placed at the center of a cubic simulation box, and a steepest descent energy minimization in vacuum was conducted. The box was then solvated with water molecules. Steepest descent energy minimization was used to remove bad van der Waals contacts between atoms. This was followed by a series of equilibration steps of 50 fs starting at 50 K (position restraints at 250000), and going in 50 K steps toward 300 K (no position restraints) while lowering the position restraints in each step by a factor of 10 except for the last step, where it was lowered by a factor of 25. This short simulation was performed with temperature coupling (τT = 0.1 ps; Tref is equal to the simulated temperature) and no pressure coupling and used the output of the previous step as input. An additional equilibration step at 300 K with temperature coupling (τT = 0.1 ps; Tref = 300 K) and isotropic pressure coupling (τP = 0.5 ps with reference pressure of 1.01325 bar and 4.5×10^{-5} compressibility) was done for 100 fs. Following the short equilibrations, the long simulations for analyses were run for a total simulation time of 50 ns with otherwise the same specifications as the last equilibration step.

RESULTS AND DISCUSSION

Recent investigations demonstrated that *trans*-iso-α-acids (**3**), but not the corresponding cis isomers (**2**), produce the tri- and tetracyclic degradation products **4**−**8** (**Figure 2**) upon storage under hydroalcoholic conditions (*28*). To confirm the differences in the reactivity of *cis*- and *trans*-iso-α-acids in beer, a forced aging experiment was performed in the following.

Forced Aging of Beer Spiked with *cis*- or *trans*-Iso-α-acids. Authentic beer samples were spiked with equal amounts of either

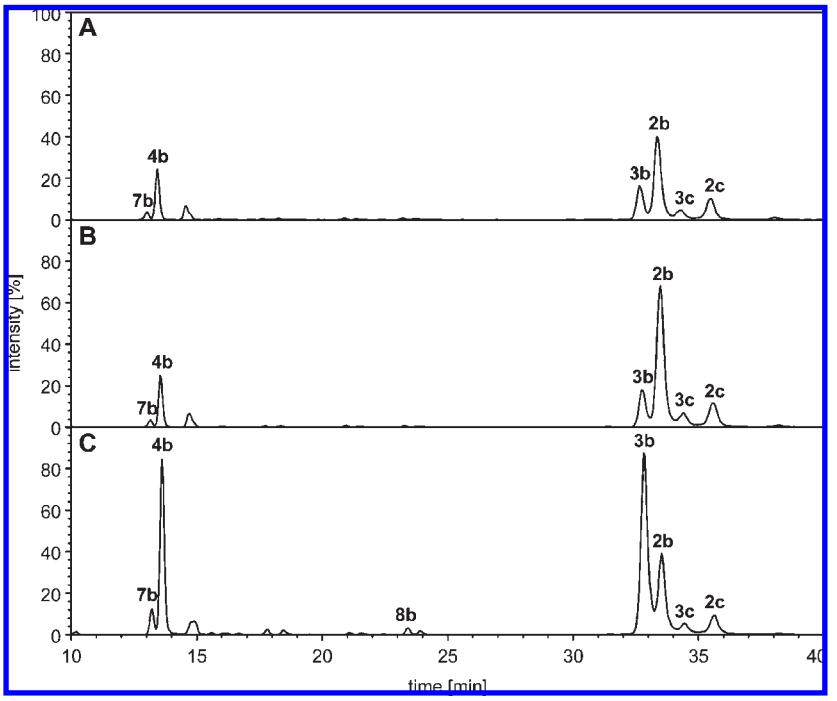

Figure 3. Excerpt of LC−MS/MS(MRM) chromatograms obtained from a beer sample maintained at 37 °C for 14 days in the absence of any additive (**A**, control), and after spiking with (**B**) *cis*-isohumulone (**2b**; 0.25 mL/2.6 μmol/L) and (**C**) *trans*-isohumulone (**3b**; 0.25 mL/3.0 μmol/L), respectively.

trans-isohumulone (**3b**) or *cis*-isohumulone (**2b**) and kept for 14 days at 37 °C in the dark. These samples as well as a control sample lacking any additive were analyzed by LC−MS/MS-MRM for the iso-α-acids **2b** and **3b** as well as the candidate degradation products **4b**−**8b**. Comparison of the MRM chromatograms showing the mass transitions tuned for the parent molecules **2b** and **3b** as well as the main degradation products tricyclohumol (**4b**), tetracyclohumol (**7b**), and epitetracyclohumol (**8b**) in the control sample (**Figure 3A**) with that of the beer samples spiked either with *cis*-isohumulone (**Figure 3B**) or with *trans*-isohumulone (**Figure 3C**) revealed that the addition of *cis*-isohumulone did only lead to the expected increase of the peak area of **2b**, but not to any increased amounts of one of the degradation products **4b**, **7b**, and **8b**, respectively. In contrast, spiking the beer with *trans*-isohumulone (**3b**) considerably induced the formation of major amounts of tricyclohumol (**4b**) and smaller amounts of tetracyclohumol (**7b**) and epitetracyclohumol (**8b**), respectively (**Figure 3C**). In addition, increased amounts of the other tricyclic products **5b** and **6b** were observed (data not shown). It is interesting to notice that spiking the beer either with the *trans*- or the *cis*-iso-α-acid did not result in the formation of one or the other stereoisomer of the iso-α-acid, thus demonstrating that these isomers do not undergo epimerization upon beer storage.

^{18}O Stable Isotope Labeling Experiments. As preliminary experiments demonstrated that *trans*-iso-α-acids (**3**) are transformed into tri- and tetracyclic degradation products **4**−**8** only in aqueous or water/alcohol solutions but not in the absence of any water (data not shown), ^{18}O-labeling experiments were performed to visualize the incorporation of oxygen atoms from water into the target molecules by means of LC−MS/MS and to gain first insights into the transformation mechanism. In order to enable the detection of ^{18}O-enriched atoms in the target molecules, first the complex MS fragmentation pattern of *trans*-isohumulone (**3b**) was to be decoded. To achieve this, the daughter ions generated by an MS/MS experiment were compared to those observed for the congener **3a** (**Table 2**). The data clearly showed that the major fragmentation routes are identical for all iso-α-acid congeners as the fragment ions detected for the different isomers differed by 14 amu, thus reflecting the structural differences in the alkanoyl side chain of the congeners. In contrast, the daughter ion *m*/*z* 235 was found independent of the congener analyzed, thus indicating that the formation of this fragment involves the cleavage of the variable alkanoyl side chain. Based on these considerations, the daughter ion *m*/*z* 235 as well as the fragment *m*/*z* 265, resulting from the cleavage of the isohexenoyl moiety, were used to read out the following ^{18}O stable isotope incorporation experiments (**Figure 4**).

After the considerations on the MS fragmentation pattern of iso-α-acids, a ^{16}O/^{18}O isotope exchange experiment (expt A) was performed in order to differentiate the stably bound oxygen atoms in the target molecule from those which undergo ^{16}O/^{18}O isotope exchange in the presence of water. Using *trans*-isohumulone (**3b**), tricyclohumol (**4b**), tricyclohumene (**5b**), isotricyclohumene (**6b**), and tetracyclohumol (**7b**) as examples, these compounds were dissolved in $H_2{}^{18}O$, the pH value was adjusted to 4.0, and then the samples were incubated for 2 h at 37 °C. Thereafter, the solutions were diluted with the nonprotic solvent acetonitrile to prevent a re-exchange of the incorporated ^{18}O atoms and were then injected into the mass spectrometer operating in the negative electrospray ionization mode, in order to study the ratio of the isotopologues as well as the fragmentation pattern of the corresponding target compounds. In a complementary ^{18}O incorporation experiment (expt B), the transformation of compounds **3b**−**7b** was performed in a solution of $H_2{}^{18}O$ in order to visualize the stable insertion of ^{18}O atoms from water into the *trans*-iso-α-acid degradation products. To achieve this, a solution (pH 2.0) of *trans*-isohumulone (**3b**) in $H_2{}^{18}O$ was incubated for 4 h at 60 °C and, after separation of the solvent in vacuum, the residue was taken up in H_2O to re-exchange labile bound ^{18}O atoms and, then, used for LC−MS/MS scan and fragmentation experiments (**Table 2**).

Incubation of **3b** in $H_2{}^{18}O$ led to a 100% incorporation of one ^{18}O atom into the molecule (**Table 2**, expt A). With the exception of *m*/*z* 235, all other fragment ions showed an isotope shift by 2 amu due to the presence of one ^{18}O atom, thus demonstrating

Table 2. Isotopologues and MS Fragments Detected for Natural ^{18}O-Abundant **3a**/**b**/**c**, **4b**, and **7b**, after $^{16}O/^{18}O$ Exchange (Expt A[a]), and after ^{18}O Incorporation (Expt B[b])

compound (no.[c])	$[M-H]^-$ $[m/z]$[d]	MS/MS fragment ions $[m/z]$[e]
trans-isocohumulone (**3a**)		
natural ^{18}O abundance	347 (100)	347, 329, 278, 251, 235, 233, 209, 207, 182, 181
trans-isoadhumulone (**3c**)		
natural ^{18}O abundance	361 (100)	361, 343, 292, 265, 247, 235, 223, 221, 196, 195
trans-isohumulone (**3b**)		
natural ^{18}O abundance	361 (100)	361, 343, 292, 265, 247, 235, 223, 221, 196, 195
after $^{16}O/^{18}O$ exchange (expt A)	363 (100)	363, 345, 294, 267, 249, 235, 225, 223, 198, 197
after ^{18}O incorporation (expt B)	361 (70)	361, 343, 292, 265, 247, 235, 223, 221, 196, 195
	363 (30)	363, 345, 294, 265, 247, 237, 225, 221, 196, 195
tricyclohumol (**4b**)		
natural ^{18}O abundance	379 (100)	379, 361, 321, 317, 303, 277, 197, 179
after $^{16}O/^{18}O$ exchange (expt A)	381 (100)	381, 363, nd, 319, 305, 277, 199, 181
after ^{18}O incorporation (expt B)	381 (70)	381, 363, 321, 319, nd, 279, 197, 179
	383 (30)	383, 365, 323, nd, nd, 281, 197, 181
tricyclohumene (**5b**)		
natural ^{18}O abundance	361 (100)	361, 343, 299, 259, 197, 179
after $^{16}O/^{18}O$ exchange (expt A)	363 (>90)	363, 345, 301, 259, 199, 181
after ^{18}O incorporation (expt B)	361 (70)	361, 343, 299, 259, 197, 179
	363 (30)	363, 345, nd, nd, nd, 179
isotricyclohumene (**6b**)		
natural ^{18}O abundance	361 (100)	361, 343, 299, 259, 197, 179
after $^{16}O/^{18}O$ exchange (expt A)	363 (>90)	363, 345, 301, 259, 199, 181
after ^{18}O incorporation (expt B)	361 (70)	361, 343, 299, 259, 197, 179
	363 (30)	363, 345, 301, 261, 197, 179
tetracyclohumol (**7b**)		
natural ^{18}O abundance	379 (100)	379, 361, 321, 303, 277, 207, 197, 179
after $^{16}O/^{18}O$ exchange (expt A)	379 (70)	379, 361, 321, 303, 277, 207, 197, 179
	381 (30)	381, 363, 323, 305, 277, 209, 197, 181
after ^{18}O incorporation (expt B)	383 (70)	383, nd, 323, 305, nd, 209, 199, 181
	385 (30)	385, 365, 325, 307, nd, 211[f], 209[f], nd, 181

[a] The target compound dissolved in $H_2{}^{18}O$ (pH 4.0) was incubated at 37 °C for 2 h and then directly analyzed by LC−MS/MS (ESI^-). [b] Solution of the pure *trans*-isohumulone (**3b**; 30 μmol/L) in $H_2{}^{18}O$ (pH 2.0) was kept for 4 h at 60 °C in the dark, the solvent was removed in vacuum, and the residue was taken up in H_2O and then analyzed by means of LC−MS/MS (ESI^-). [c] Structures and numbering of compounds refer to **Figures 1** and **2**. [d] Pseudomolecular ion found for each ^{18}O isotopologue of the target compound; relative abundance in % is given in parentheses. [e] Mass spectrometric fragment ions observed upon MS/MS using collision activated dissociation. [f] Mixture of isotopologues in a certain fragment ion; nd: not detected due to low abundancy.

the incorporation of the ^{18}O label into the tricarbonyl system of **3b**. In contrast, the MS/MS analysis of **3b** in expt B revealed that only 30% of the molecules are ^{18}O labeled (**Table 2**). Careful assignment of the MS/MS fragments implied that the ^{18}O atom is incorporated at the carbonyl atom C1′ of the isohexenoyl chain. It is interesting to notice that the isolated carbonyl group in the isohexenoyl moiety does undergo a 30% $^{16}O/^{18}O$ exchange under more severe acidic conditions (expt B), but not under the mild conditions applied in expt A.

As found for **3b**, also the $^{16}O/^{18}O$ exchange experiment (expt A) performed with tricyclohumol (**4b**) resulted in a 100% insertion of one ^{18}O atom into the tricarbonyl system as confirmed by fragment ion m/z 277 (**Table 2**). In contrast, after transformation of **3b** into **4b** in the presence of $H_2{}^{18}O$, a mixture of 70% singly ^{18}O labeled (m/z 381) and 30% twice ^{18}O labeled isotopologues of 4b (m/z 383) was found. Fragmentation of the pseudomolecular ion m/z 381 revealed the nonlabeled daughter ion m/z 321 upon cleavage of the hydroxypropyl moiety at C3′ (**Figure 4**), thus demonstrating that the newly formed hydroxyl function in **4b** originates from water. This was also found for the $[^{18}O_2]$-isotopologue with the pseudomolecular ion m/z 383. As already shown above for the precursor **3b**, the conditions applied in expt B revealed a 30% $^{16}O/^{18}O$ exchange of the carbonyl oxygen of the isohexenoyl moiety in the $[^{18}O_2]$-labeled compound **4b**, thus indicating that the hydroxy function at C1′ of **4b** is originating from the former carbonyl of the isohexenoyl moiety in **3b**. This conclusion is also supported by the observation that the tricyclic derivatives **5b** and **6b**, respectively, showed a 30% enrichment of a single ^{18}O atom (**Table 2**).

LC−MS/MS analysis of tetracyclohumol (**7b**) obtained in expt B revealed a mixture of 70% double ^{18}O labeled (m/z 383) and 30% triple ^{18}O labeled isotopologues of **7b** (m/z 385), thus indicating the presence of two 100% ^{18}O enriched oxygen atoms in **7b** and again a 30% ^{18}O enrichment of the hydroxyl function at C1′ as found for **4b**. One of the 100% labeled oxygen atoms could be assigned as one of the hydroxyl function at C(3″) within a hydroxypropyl moiety, thus indicating that this hydroxyl group originates from water. The position of the remaining ^{18}O atom could not be unambiguously assigned. As two oxygen atoms of the tricarbonyl system of **3b** seem to be involved in the formation of **7b** and the results of the incubation experiments of **3b** showed that one of these carbonyls undergoes 100% $^{16}O/^{18}O$ exchange, it might be concluded that either the hydroxyl group at C3 or the hydroxyl function at C1‴ is ^{18}O labeled (**Figure 4**). The eye-catching observation that one hydroxyl oxygen in all the degradation products showed a $^{16}O/^{18}O$ exchange rate of exactly 30% gives strong evidence that the formation of the tricyclic and tetracyclic degradation products from **3b** runs via a common reaction mechanism.

Influence of Temperature and pH Value on the Formation of 4−8 from *trans*-Iso-α-acids. In order to answer the question as to whether the formation of compounds **4**−**8** from **3** requires oxidative or photooxidative reaction steps involving air oxygen, canned beer with a very low oxygen content of less than 0.1 mg/L (< 3.1 μmol/L) were maintained at 6, 27, and 37 °C for up to 18 weeks and, then, analyzed for the degradation products **4**−**8** by means of LC−MS/MS. The time-dependent decrease of *trans*-isocohumulone (**3a**) and the increase of the amounts of products

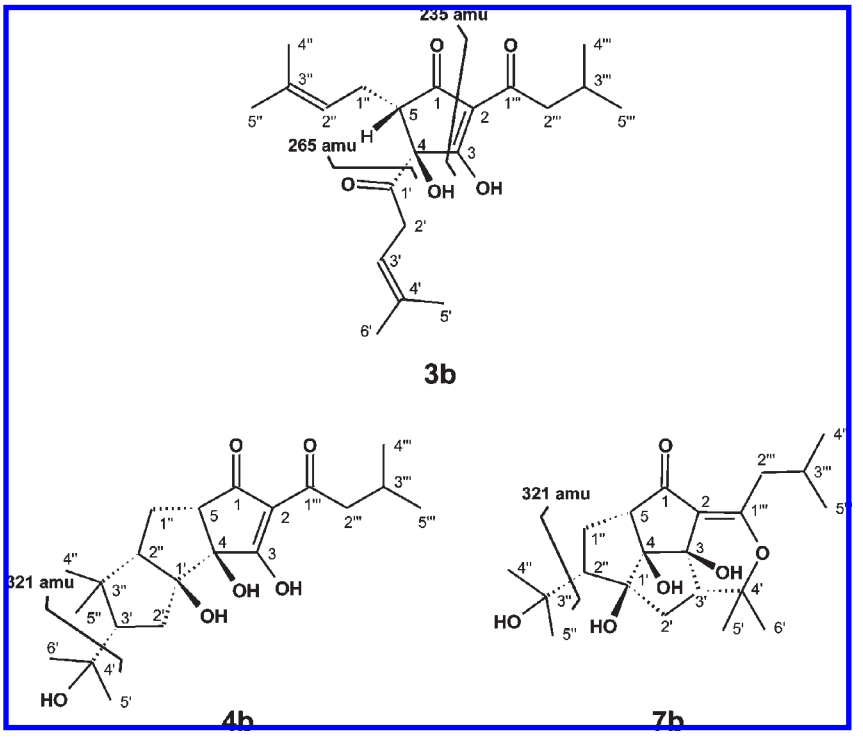

Figure 4. Proposed key fragment ions of *trans*-isohumulone (**3b**), tricyclohumol (**4b**), and tetracyclohumol (**7b**) identified by MS/MS experiments.

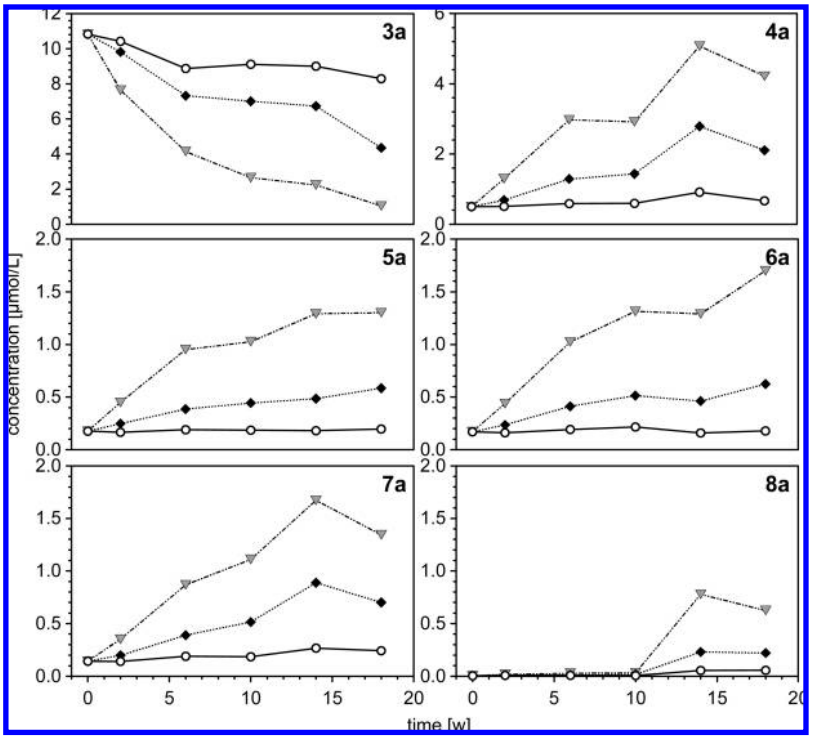

Figure 5. Degradation of *trans*-isocohumulone (**3a**) and formation of the degradation products **4a**−**8a** upon storage of canned beer at 6 °C (○), 27 °C (◆), and 37 °C (▼), respectively. Experiment was carried out in triplicate (calculated relative standard deviation <10%).

(**4a**−**8a**) are displayed in **Figure 5**. Keeping the beer samples at 6 °C did only marginally influence the concentrations of the target compounds, e.g. after 18 weeks only 20% of **3a** was degraded and the formation of **4**−**8** could hardly be detected. In comparison, maintaining the beer at 37 °C induced a strong degradation of the parent *trans*-iso-α-acid **3a** accompanied by the generation of **4a**−**8a**, e.g. after 18 weeks almost all of the *trans*-iso-α-acid was gone (**Figure 5**). Besides the loss of 11 µmol/L of *trans*-isocohumulone (**3a**), the degradation products **4a**−**8a** were observed to be generated with a rather similar temperature-dependent formation rate leading to concentrations of 1−5 µmol/L after 18 months. After this reaction time, tricyclocohumol (**4a**) was found as the most predominant and epitetracyclocohumol (**8a**) as the minor reaction product. The total concentration of all the degradation products **4a**−**8a** formed from 11 µmol/L *trans*-isocohumulone (**3a**) accounted for about 10 µmol/L, thus demonstrating that 91% of the *trans*-iso-α-acid

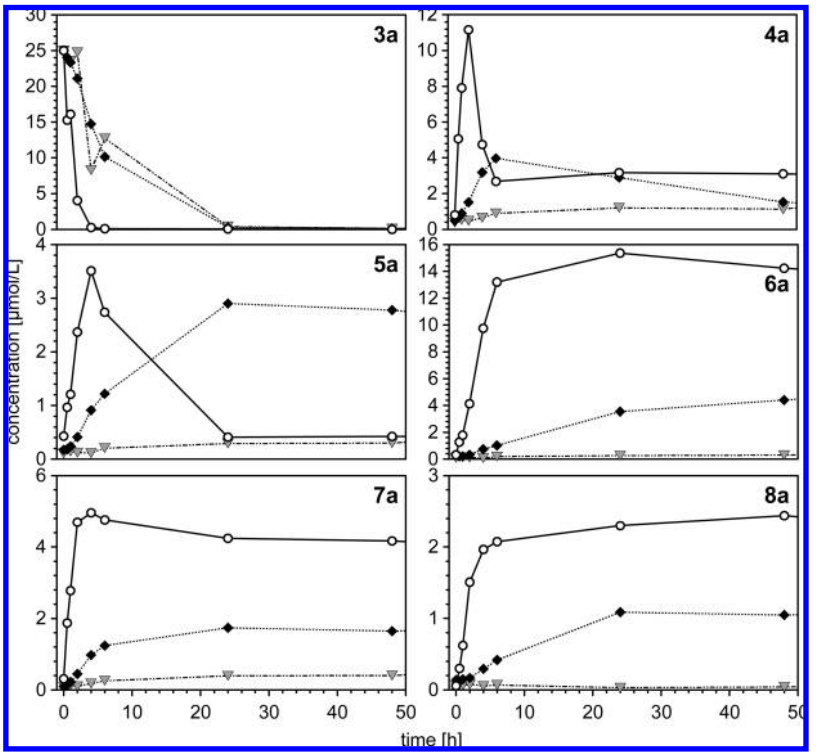

Figure 6. Degradation of *trans*-isocohumulone (**3a**) and formation of compounds **4a**−**8a** in aqueous solution (60 °C) at pH 1.0 (○), pH 3.0 (◆), and 4.0 (▼), respectively. Experiment was carried out in triplicate (calculated relative standard deviation <10%).

degradation could be elucidated on a molecular level. As these experiments were performed with canned beer under quasi oxygen-free conditions in the absence of light, it can be concluded that oxidative and/or photooxidative reactions do not play any major role in the transformation of *trans*-iso-α-acids into the lingering and harsh bitter compounds **4**−**8**.

In order to investigate whether the formation of compounds **4**−**8** from **3** runs via proton-catalyzed reactions, aqueous solutions of *trans*-isocohumulone (**3a**) adjusted to pH 1.0, 3.0, 4.0, and 6.0, respectively, were incubated at 60 °C for up to 50 h under an atmosphere of nitrogen and were then analyzed by means of LC−MS/MS. As shown in **Figure 6**, the degradation of **3a** and the formation of **4a**−**8a** were found to be strongly pH-dependent. The most rapid degradation of **3a** to compounds **4a**−**8a** was observed at pH 1.0, e.g. less than 5% of **3a** remained already after 4 h. At this low pH value, the tricyclic products tricyclocohumol (**4a**) and tricyclocohumene (**5a**) were then formed most rapidly running through a maximum of 11.2 and 3.5 μmol/L after a reaction time of 2 and 4 h, respectively. In comparison, the concentration of isotricyclocohumene (**6a**) increased somewhat more slowly and reached its maximum concentration of 15.2 μmol/L after 24 h. Interestingly, the total amount of the three tricycles **4a**−**6a** was found to be rather constant while the ratio between the individual components changed drastically until an equilibrium was reached after 24 h (**Figure 6**). Surprisingly, compound **6a** was found to be formed with increasing reaction time of up to 50 h, although the precursor compound **3a** was already consumed after 4 h. This observation clearly implies that isotricyclocohumene (**6a**) is formed by transformation of tricyclocohumol (**4a**) and tricyclocohumene (**5a**) detected as major reaction products already after short reaction times. In addition, the experiment performed at pH 1.0 showed that the tetracycles **7a** and **8a** are preferentially generated within the first 4 h of the reaction and, in contrast to **4a** and **5a**, did change only slightly with increasing reaction time. Increasing the pH value to 3.0 and, in particular, to 4.0

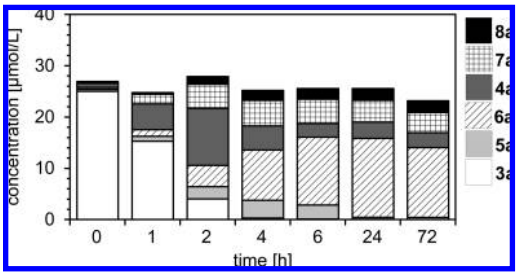

Figure 7. Influence of the reaction time on the concentrations of *trans*-isocohumulone (**3a**), tricyclocohumol (**4a**), tricyclocohumene (**5a**), isotricyclocohumene (**6a**), tetracyclocohumol (**7a**), and epitetracyclocohumol (**8a**) in aqueous solution (pH 1.0, 60 °C).

induced a significant decrease of the reaction speed, whereas none of these compounds were formed at pH 6.0 within the considered time range (data not shown), thus demonstrating a strong influence of the pH value on the formation of **4**−**8** from *trans*-iso-α-acids. As shown in the stacked bar plot in **Figure 7**, the total amount of the precursor **3a** and the corresponding degradation products **4a**−**8a** accounted for more than 90% of the starting material independent of the reaction time (pH 1.0), thus implying that the transformation of **3a** into **4a**−**8a** is following a rather specific and quantitative reaction.

Reaction Mechanism Proposed for the Formation of 4−8 from *trans*-Iso-α-acids. Based on the findings obtained from the ^{18}O-labeling studies and quantitative model experiments, a reaction pathway was proposed for a proton-catalyzed, intramolecular nucleophilic cyclization of *trans*-iso-α-acids (**3**) giving rise to the degradation products **4**−**8** (**Figure 8**). Protonation of the carbonyl group of the isohexenoyl side chain in **3** leads to the intermediary carbocation 1, which undergoes cyclization by an intramolecular attack of the π-electrons of the methine carbon of the prenyl chain, thus giving rise to the carbocation 2. This intermediate (2) might

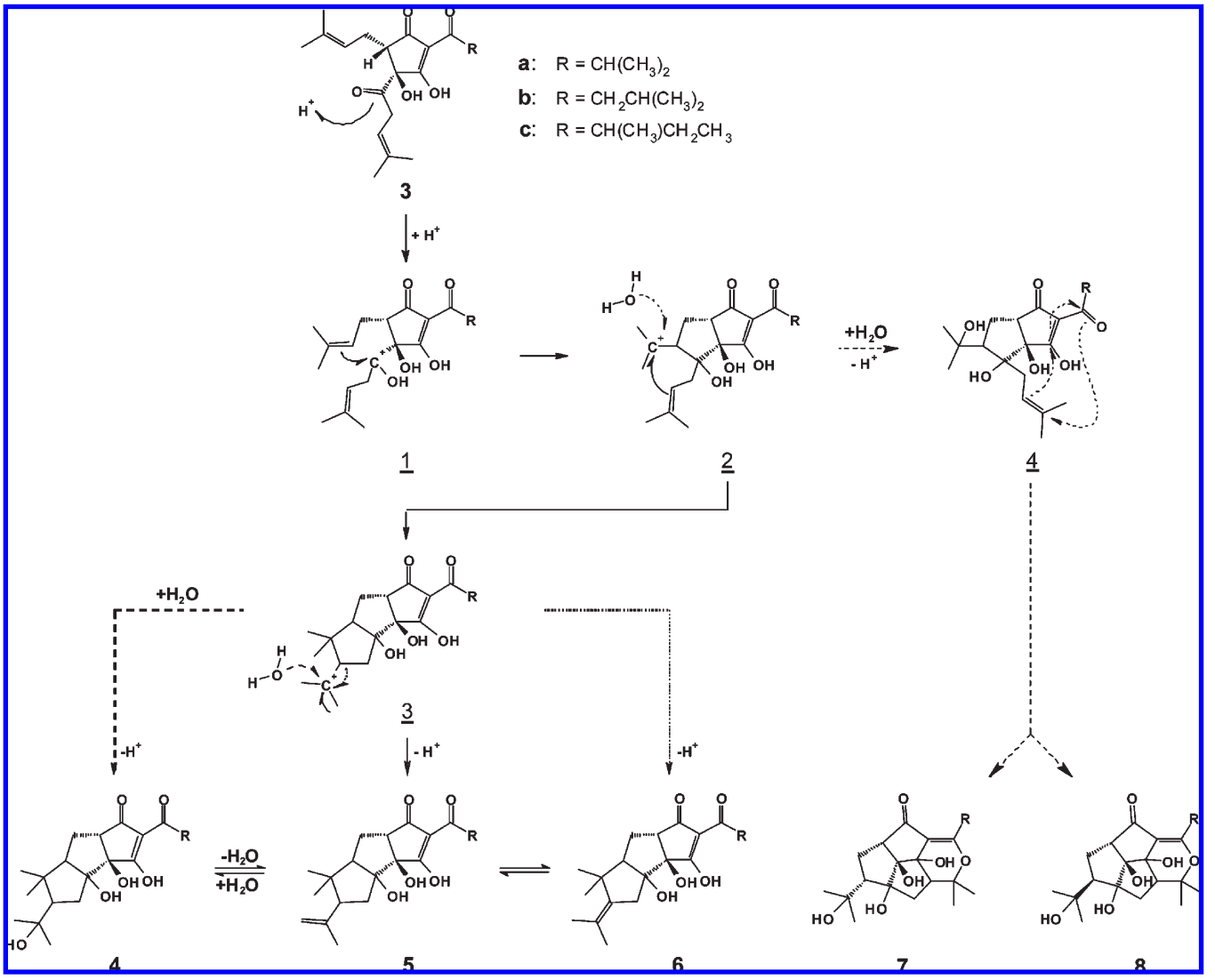

Figure 8. Proposed reaction mechanism explaining the formation of the tricyclic (**4**, **5**, **6**) and tetracyclic degradation products (**7**, **8**) from *trans*-iso-α-acids (**3**).

undergo a second intramolecular attack of the olefinic carbon of the isoprenyl side chain to give the carbocation 3, which can further react to stable end products via three alternative routes. Nucleophilic addition of a molecule of water leads to the formation of the alcohol **4**, whereas elimination of a proton gives rise to the unsaturated compounds **5** and **6**, respectively. As shown by quantitative model studies (**Figure 6**), the tricycles **4**, **5**, and **6** were found to be converted into each other, thus reaching a molar equilibrium ratio of 6:1:30. Alternatively, carbocation 2 might add water to give the intermediary alcohol 4. Protonation of 4 at the carbonyl function of the alkanoyl side chain then induces an intramolecular cyclization involving the double bond of the isoprenyl side chain as well as vinylogous carbonyl moiety in the tricarbonyl system. Depending on the initial configuration of the intermediate 2, either the tetracycle **7** or **8** is formed (**Figure 8**).

Stereochemical Considerations Using Molecular Dynamics Simulations. In order to further strengthen the mechanisms proposed above and to answer the question as to why exclusively the *trans*-iso-α-acids (**3**) but not the *cis*-iso-α-acids (**2**) are able to generate compounds **4**−**8**, molecular dynamics simulations were conducted. To achieve this, the molecules of *cis*- (**2a**) and *trans*-isocohumulone (**3a**) were simulated in water at 27 °C for 50 ns and the distance and relevant angles at the initial cyclization site of both molecules were analyzed (see Supporting Information). These calculations show that both molecules exist in a state with

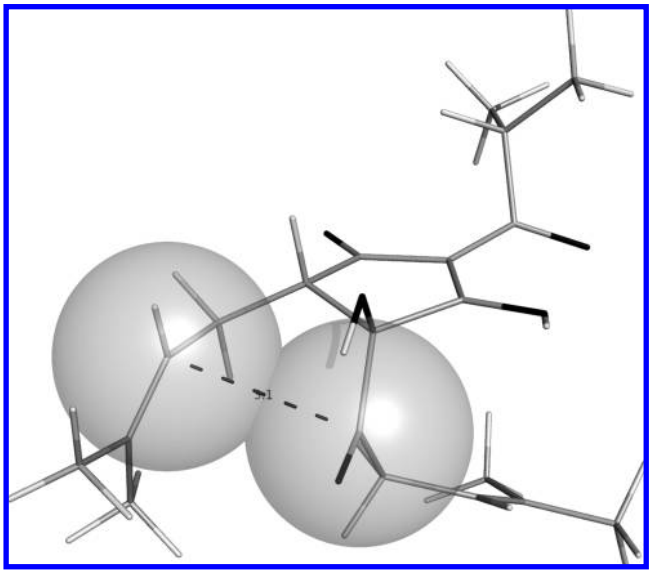

Figure 9. *trans*-Isocohumulone (**3a**) with the shortest C(1′)−C(2″) distance of 3.1 Å taken directly from the molecular dynamics trajectory. The transparent spheres indicate the van der Waals radii of the target atoms C(1′) and C(2″).

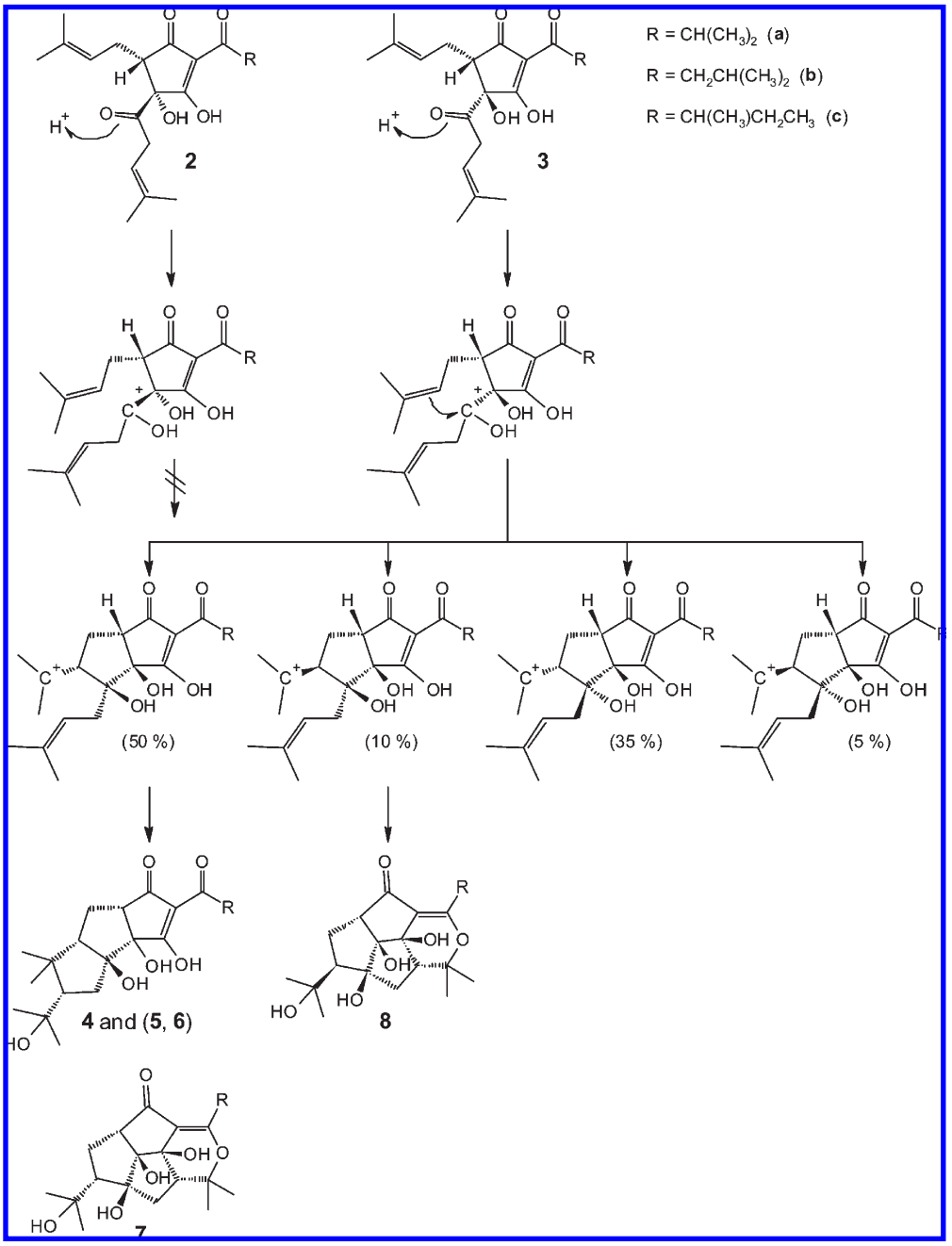

Figure 10. Reaction scheme explaining the degradation probability of *cis*- (**2**) and *trans*-iso-α-acids (**3**). The four possible stereoisomeric intermediates formed from **3** after the first cyclization step as well as the resulting degradation products **4**−**8** are shown. The relative distribution of the conformations of the precursor molecule **3** was extracted from the molecular dynamics simulation and is given in parentheses.

maximum distance between atoms C(1′) and C(2″) as well as in a state in which both atoms come closer than 4 Å. For the trans isomer (**3a**), the atoms are >2.5 times more frequent (7.9% of total time) in the latter stage when compared to **2a**. Additionally, the mean distance of the atoms C(1′) and C(2″) is about 0.18 Å higher for **2a** due to the cis configuration of the hydroxyl group at C(4) and carbon chain C(1″−5″) bound to the five-membered ring of the isocohumulone. Only for *trans*-isocohumulone (**3a**), the target carbon atoms C(1′) and C(2″) (**Figure 4**) can approximate as far as their van der Waals radii allow and, furthermore, only the steric geometry shown for **3a** enables an overlapping of the corresponding π-orbitals of these target carbons (**Figure 9**). Being well in line with the experimental finding that exclusively the *trans*-iso-α-acids are degraded during storage in hydroalcoholic solutions as well as beer samples (*21*, *28*), both steric and dynamics aspects give evidence that the formation of a novel carbon/carbon bond between C(1′) and C(2″) is more likely for the trans isomer **3a** rather than for the cis isomer **2a**.

The molecular dynamics trajectory of **3a** was then analyzed in more detail to elucidate the stereocenters and their configurations in the emerging products. Hence, the relevant dihedral angles of the carbonyl (C(1′)) and the alkene group (C(2″)) relative to the plane of the five-membered ring were examined. The carbonyl oxygen of the isohexenoyl moiety has a tendency (about 60% of the time when the atoms are in close proximity [59.24%]) to point into the same direction as the hydroxyl group at C(4) of the initial ring system, which could be attributed to a possible hydrogen bond between these two groups (**Figure 9**). This is also in agreement with experimental data as all compounds studied so far show this configuration at the carbon of the former keto function (*28*).

The methine proton H−C(2″) of the prenyl side chain exhibits a very strong tendency (about 90%) to point into the direction of the hydroxyl group of the ring system. In this case, the calculated values of the different possible configurations, represented by the relative temporal frequency of the *trans*-isocohumulone conformations from molecular dynamics simulation, are in good agreement with the distribution of substances observed in the pH-dependent model experiments performed above (**Figure 7**). As shown in **Figure 10**, the majority of the identified compounds (**4**−**7**) exhibit the relative configuration corresponding to the most likely conformation (∼50%) and only a single product (**8**) was found to be formed with another conformation.

In summary, application of ^{18}O stable isotope labeling as well as quantitative model experiments, followed by computer-based simulations, revealed for the first time a conclusive mechanism explaining the stereospecific transformation of *trans*-iso-α-acids (**2**) into the tri- and tetracyclic compounds **4**−**8**. This transformation was proposed to be induced by a proton-catalyzed carbon/carbon bond formation between the carbonyl atom C(1′) of the isohexenoyl moiety and the alkene carbon C(2″) of the isoprenyl moiety of **2**. The findings that pH value and temperature are important triggers of the undesirable transformation of *trans*-iso-α-acids will be helpful for the brewing industry to develop appropriate tools to increase the flavor shelf life of beer and hop-containing beverages.

ACKNOWLEDGMENT

We are grateful to the Hallertauer Hopfenveredelungsgesellschaft mbH (Mainburg, Germany) for providing hop samples.

Supporting Information Available: Frequency of distances between the carbonyl atom C(1′) and the alkene carbon C(2″) of the isoprenyl moiety that cyclize in the first reaction step of compounds **2** and **3** extracted from the molecular dynamics simulation. This material is available free of charge via the Internet at http://pubs.acs.org.

LITERATURE CITED

(1) Intelmann, D.; Batram, C.; Kuhn, C.; Haseleu, G.; Meyerhof, W.; Hofmann, T. Three TAS2R bitter taste receptors mediate the psychophysical responses to bitter compounds of hops (*Humulus lupulus* L.) and beer. *Chemosens. Percept.* **2009**, *2*, 118–132.

(2) De Keukeleire, D.; Verzele, M. The absolute configuration of the isohumulones and the humulinic acids. *Tetrahedron* **1971**, *27*, 4939–4945.

(3) Kowaka, M.; Kokubo, E. Composition of bitter substances of hops and characteristics of beer bitterness. *J. Am. Soc. Brew. Chem.* **1976**, *35*, 16–21.

(4) Malowicki, M. G.; Shellhammer, T. H. Isomerization and degradation kinetics of hop (*Humulus lupulus*) acids in a model wort-boiling system. *J. Agric. Food Chem.* **2005**, *53*, 4434–4439.

(5) Jaskula, B.; Kafarski, P.; Aerts, G.; De Cooman, L. A kinetic study on the isomerization of hop α-acids. *J. Agric. Food Chem.* **2008**, *56*, 6408–6415.

(6) Araki, S.; Takashio, M.; Shinotsuka, K. A new parameter for determination of the extent of staling in beer. *J. Am. Soc. Brew. Chem.* **2002**, *60*, 26–30.

(7) Masuda, S.; Kikuchi, K.; Harayama, K. Determination of light-struck character in beer by gas chromatography-mass spectroscopy. *J. Am. Soc. Brew. Chem.* **2000**, *58*, 152–154.

(8) Vanderhaegen, B.; Delvaux, F.; Daenen, L.; Verachtert, H.; Delvaux, F. R. Aging characteristics of different beer types. *Food Chem.* **2007**, *103*, 404–412.

(9) Burns, C. S.; Heyerick, A.; De Keukeleire, D.; Forbes, M. D. E. Mechanism for formation of the lightstruck flavor in beer revealed by time-resolved electron paramagnetic resonance. *Chem.—Eur. J.* **2001**, *7*, 4553–4561.

(10) Huvaere, K.; Andersen, M. L.; Olsen, K.; Skibsted, L. H.; Heyerick, A.; De Keukeleire, D. Radicaloid-type oxidative decomposition of beer bittering agents revealed. *Chem.—Eur. J.* **2003**, 4693–4699.

(11) Schieberle, P. Primary odorants of pale lager beer. Differences to other beers and changes during storage. *Z. Lebensm.-Unters. -Forsch.* **1991**, *193*, 558–565.

(12) De Keukeleire, D.; Heyerick, A.; Huvaere, K.; Skibsted, L. H.; Andersen, M. L. Beer lightstruck flavor: the full story. *Cerevisia* **2008**, *33*, 133–144.

(13) Vanderhaegen, B.; Neven, H.; Verachtert, H.; Derdelinckx, G. The chemistry of beer aging - a critical review. *Food Chem.* **2006**, *95*, 357–381.

(14) De Cooman, L.; Aerts, G.; Overmeire, H.; De Keukeleire, D. Alterations of the profiles of iso-α-acids during beer ageing, marked instability of trans-iso-α-acids and implications for beer bitterness consistency in relation to tetrahydroiso-α-acids. *J. Inst. Brew.* **2000**, *106*, 169–178.

(15) Pangborn, R. M.; Lewis, M. J.; Tanno, L. S. Sensory quantification of bitterness and flavour of beer during storage. *J. Inst. Brew.* **1977**, *83*, 244–250.

(16) King, B. M.; Duineveld, C. A. A. Changes in bitterness as beer ages naturally. *Food Qual. Pref.* **1999**, *10*, 315–324.

(17) Hughes, P. S.; Menneer, I. D.; Walters, M. T.; Marinova, G. Differential behaviour of cis- and trans-iso-α-acids. *Proc. 27th EBC Congr.* **1997**, *26*, 231–238.

(18) Malfliet, S.; Van Opstaele, F.; De Clippeleer, J.; Syryn, E.; Goiris, K.; De Cooman, L.; Aerts, G. Flavour instability of pale lager beers: Determination of analytical markers in relation to sensory ageing. *J. Inst. Brew.* **2008**, *114*, 180–192.

(19) Jaskula, B.; Syryn, E.; Goiris, K.; De Rouck, G.; Van Opstaele, F.; De Clippeleer, J.; Aerts, G.; De Cooman, L. Hopping technology in relation to beer bitterness consistency and flavor stability. *J. Am. Soc. Brew. Chem.* **2007**, *65*, 38–46.

(20) De Cooman, L.; Aerts, G.; Witters, A.; De Ridder, M.; Boeykens, A.; Goiris, K.; De Keukeleire, D. Comparative study of the stability of iso-α-acids, dihydroiso-α-acids and tetrahydroiso-α-acids during beer ageing. *Cerevisia* **2001**, *26*, 155–160.

(21) Intelmann, D.; Haseleu, G.; Hofmann, T. LC-MS/MS Quantitation of hop-derived bitter compounds in beer using the ECHO technique. *J. Agric. Food Chem.* **2009**, *57*, 1172–1182.

(22) Diffor, D. W.; Ramos, E. S. A.; Hansen, G. L. Preparation of humulinic acid. Effect on analytical and flavor characteristics of beer. *Proc. Am. Soc. Brew. Chem.* **1972**, 109–114.

(23) Schulze, W. G.; Ting, P. L.; Henckel, L. A.; Goldstein, H. Separation of humulinic acids by reverse-phase high performance liquid chromatography. *J. Am. Soc. Brew. Chem.* **1981**, *39*, 12–15.

(24) Vanhoey, M.; Vandewalle, M.; Verzele, M. Oxidation products of isohumulones. *Bull. Soc. Chim. Belg.* **1970**, *79*, 499–509.

(25) Clarke, B. J.; Hildebrand, R. P. The isomerization of humulone; III. The degradation of isohumulone. *J. Inst. Brew.* **1967**, *73*, 282–293.

(26) De Keukeleire, D. Oxidation products from hop-α-acids and iso-α-acids (in Dutch). *Cerevisia* **1981**, 73–80.

(27) Cann, M. R.; Davis, A.-M.; Shannon, P. V. R. New rearrangement and oxidation products from humulone. *J. Chem. Soc., Perkin Trans. 1* **1982**, 375–383.

(28) Intelmann, D.; Kummerlöwe, G.; Haseleu, G.; Desmer, N.; Schulze, K.; Fröhlich, R.; Frank, O.; Luy, B.; Hofmann, T. Structures of storage-induced transformation products of the beer's bitter principle, revealed by sophisticated NMR and LC/MS techniques. *Chem.—Eur. J.*, in press.

(29) Berendsen, H. J. C.; van der Spoel, D.; van Drunen, R. GROMACS: A message-passing parallel molecular dynamics implementation. *Comput. Phys. Commun.* **1995**, 43–56.

(30) Lindahl, E.; Hess, B.; van der Spoel, D. GROMACS 3.0: A package for molecular simulation and trajectory analysis. *J. Mol. Model.* **2001**, 306–317.

(31) Humphrey, W.; Dalke, A.; Schulten, K. VMD: Visual molecular dynamics. *J. Mol. Graphics* **1996**, 33–38.

(32) Berendsen, H. J. C.; Postma, J. P. M.; Vangunsteren, W. F.; Dinola, A.; Haak, J. R. Molecular-dynamics with coupling to an external bath. *J. Chem. Phys.* **1984**, 3684–3690.

Received for review August 26, 2009. Revised manuscript received October 5, 2009. Accepted October 5, 2009. We are grateful to Bitburger brewery for financial support.